

ORIGINAL RESEARCH



Gas plasma irradiation of breast cancers promotes immunogenicity, tumor reduction, and an abscopal effect in vivo

Hamed Mahdikia^{a,b}, Fariba Saadati^b, Eric Freund^{b,c*}, Udo S. Gaipf^d, Keivan Majidzadeh-a^e, Babak Shokri^{a,f}, and Sander Bekeschus^{b*}

^aLaser and Plasma Research Institute, Shahid Beheshti University, Tehran, Iran; ^bCenter for Innovation Competence (ZIK) Plasmatis, Leibniz Institute for Plasma Science and Technology (INP), Greifswald, Germany; ^cDepartment of General, Visceral, Thoracic and Vascular Surgery, Greifswald University Medical Center, Greifswald, Germany; ^dDepartment of Radiation Oncology, Universitätsklinikum Erlangen, Friedrich-Alexander-Universität Erlangen-Nürnberg, Erlangen, Germany; ^eRecombinant Proteins Department, Breast Cancer Research Center, Motamed Cancer Institute, ACECR, Tehran, Iran; ^fDepartment of Physics, Shahid Beheshti University, Tehran, Iran

ABSTRACT

While many new and emerging therapeutic concepts have appeared throughout the last decades, cancer still is fatal in many patients. At the same time, the importance of immunology in oncotherapy is increasingly recognized, not only since the advent of checkpoint therapy. Among the many types of tumors, also breast cancer has an immunological dimension that might be exploited best by increasing the immunogenicity of the tumors in the microenvironment. To this end, we tested a novel therapeutic concept, gas plasma irradiation, for its ability to promote the immunogenicity and increase the toxicity of breast cancer cells in vitro and in vivo. Mechanistically, this emerging medical technology is employing a plethora of reactive oxygen species being deposited on the target cells and tissues. Using 2D cultures and 3D tumor spheroids, we found gas plasma-irradiation to drive apoptosis and immunogenic cancer cell death (ICD) in vitro, as evidenced by an increased expression of calreticulin, heat-shock proteins 70 and 90, and MHC-I. In 4T1 breast cancer-bearing mice, the gas plasma irradiation markedly decreased tumor burden and increased survival. Interestingly, non-treated tumors injected in the opposite flank of mice exposed to our novel treatment also exhibited reduced growth, arguing for an abscopal effect. This was concomitant with an increase of apoptosis and tumor-infiltrating CD4⁺ and CD8⁺ T-cells as well as dendritic cells in the tissues. In summary, we found gas plasma-irradiated murine breast cancers to induce toxicity and augmented immunogenicity, leading to reduced tumor growth at a site remote to the treatment area.

ARTICLE HISTORY

Received 24 June 2020
Revised 1 December 2020
Accepted 1 December 2020

KEYWORDS

ICD; immunogenic cancer cell death; leukocytes; medical technology; oncology; plasma medicine; reactive oxygen species; ros

Introduction

Breast cancer is the most frequent type of cancer in women worldwide, with many of the cases being fatal.^{1–3} The development of efficient and new treatment methods is difficult because of the complex nature of that type of cancer.⁴ Most breast cancer-related deaths occur if metastatic cells begin to detach from the primary tumor and start to spread to surrounding tissue or secondary sites. During this process, cancer cells detach from the primary tumor by invading the basement membrane, crossing connective tissue, and penetrating other organs through blood vessels or lymphatic vessels.^{5,6} In general, novel cancer therapies should be effective, safe, and associated with a minimum of side effects.^{7,8}

There is a variety of different traditional and novel treatment options for cancer, such as surgery, chemotherapy, radiotherapy, photodynamic therapy, and immunotherapy.^{9–11} Especially the latter received increased attention during the recent years.¹² Clinical trials using immune checkpoint inhibitors in patients with triple-negative breast cancer, such as atezolizumab targeting PD-L1, showed promising results.^{13,14} This builds the case

for the power of unleashing antitumor immunity in breast cancer patients, which was observed already for other tumor entities.^{15,16} Tumor cells mutate at high frequencies, leading to an elevated mutational burden that correlates to responses to immunotherapy in patients.¹⁷ For breast cancer, on average, somatic mutations are regularly observed,¹⁸ facilitating antitumor T-cells responses for attacking metastatic lesions.

However, for antitumor immunity to form, tumor antigens not only need to be present but also accessible and processable for antigen-presenting cells to promote T-cell mediated immunity. Radiotherapy has been proven to exert immune modulatory effects.¹⁹ Locally applied ionizing radiation can thereby potentiate antitumor immunity, leading to reduced cancer growth also of distant, untreated sites (abscopal effect).²⁰ It is noteworthy that radiotherapy, to some extent, relies on the local generation of reactive oxygen species (ROS).²¹ Further, radiotherapy synergizes with other ROS-inducing treatments such as gas plasma in the induction of cancer cell death with immune stimulatory properties.²² Therapeutic levels of ROS are increasingly appreciated as novel paradigm for cancer treatment.²³

Gas plasma technology is an emerging innovation in oncology.²⁴ It is recognized that the main mode of action of these partially ionized gases operated at body temperature relies on the generation of ROS.²⁵ The unique feature of gas plasma systems is that a plethora of different types of ROS is being produced simultaneously,²⁶ facilitating oxidative damage of tumor cells and, ultimately, leading to their demise. While the concept of ROS-mediated killing using gas plasmas has been explored to some extent,²⁷ the immunological consequences of gas plasma irradiation of breast cancer cells are unknown. To this end, we investigated gas plasma-irradiated breast cancer cells in terms of toxicity and immunogenicity *in vitro* and *in vivo*. Gas plasma irradiation not only effectively controlled tumor growth but also was concomitant with an upregulation of several markers of the immunogenic cancer cell death (ICD), such as calreticulin (CRT) and the damage-associated molecular pattern (DAMP) molecules heat-shock protein (HSP) 70 and HSP90.^{28,29} Finally, we found gas plasma irradiation to mediate an abscopal effect in breast-cancer bearing mice, mounting evidence of a promising role of therapeutic ROS derived from gas plasma systems in promoting anticancer immunity.

Materials and methods

Cell culture and *in vitro* gas plasma irradiation

Human breast cancer cell lines MCF-7 (ATCC: HTB-22) and MDA-MB (ATCC: HTB-26) were cultivated in Dulbecco's Modified Eagles' Medium (DMEM; Corning). The murine breast cancer cell line 4T1 (ATCC: CRL-2539) was cultured in Roswell Park Memorial Institute (RPMI) 1640 medium (Corning). All culture media were supplemented with 10% fetal bovine serum, 2% L-glutamine, and 1% penicillin (all Sigma Aldrich), and were kept under standard culture conditions at 37°C, 5% CO₂, and 95% humidity in a cell culture incubator (Binder). Twenty-four hours before experiments, the cells were seeded at 5×10^4 cells per ml of fully supplemented medium in 24-well tc-treated cell culture plates (Eppendorf). Three-dimensional tumor spheroids were formed as described before.³⁰ Briefly, cells were seeded at 4×10^3 cells per 200 μ l fully supplemented medium in 96-well ultra-low attachment plates (Corning). After centrifugation at 1000 x g for 10 min, the cells were cultured for 72 h before experiments. For the gas plasma irradiation of the cells *in vitro*, a helium-driven plasma jet was utilized. Its technical parameters and physical properties have been described in detail before.²⁶ It was operated with a gas flow four standard liters helium (purity: 99.999%; Air Liquide). The distance of the target to plasma as well as the treatment time was kept constant using a software-controlled xyz-table (CNC Step). Vehicle controls received helium gas only, through the same system.

Reactive species detection

For the detection of reactive species introduced into the cell culture medium following gas plasma irradiation, several different assays were applied. Hydrogen peroxide (H₂O₂) was quantified utilizing the Amplex Ultra Red assay kit (ThermoFisher) according to the manufacturers' instructions.

For the detection of nitrite (NO₂⁻) inside the medium, a deterioration product of nitric oxide (NO), the Griess assay (Cayman Chemical) was carried out. Hypochlorous acid (HOCl) was detected by the colorimetric taurine chloramine assay, as previously described.³¹ The measurements were performed using a multiplate reader (Tecan Infinite F200 PRO) at $\lambda_{\text{ex/em}} = 535 \text{ nm}/590 \text{ nm}$ for fluorescence detection (H₂O₂), or the (Tecan Infinite M200 PRO) at $\lambda = 540 \text{ nm}$ (NO₂⁻) and at $\lambda = 645 \text{ nm}$ (HOCl) for absorbance detection. The pH levels of gas plasma-irradiated cell culture medium were quantified using a pH-meter (Mettler Toledo).

Metabolic activity and cytotoxicity

Resazurin (Alfa Aesar), a non-fluorescent dye becoming fluorescent after reduction via cell-derived NADPH, was added at 22 h or 46 h after gas plasma irradiation at a final concentration of 100 μ M and incubated for 2 h. Fluorescence was detected by a multimode plate reader (Tecan Infinite F200 PRO) at $\lambda_{\text{ex}} 535 \text{ nm}$ and $\lambda_{\text{em}} 590 \text{ nm}$. For assessing cytotoxicity via microscopy, 4,6-Diamidin-2-phenylindol (DAPI, final concentration 1 μ M; BioLegend) was added to each well. Subsequently, the cells were imaged using a high-content imaging analysis system (Operetta CLS; PerkinElmer) with a 20x (NA = 0.4) air objective (Zeiss) equipped with laser-based autofocus (785 nm). Imaging was performed using the brightfield channel (with a 740 nm transmission light source), the digital phase contrast (DPC) channel (generating a single image from differential contrasts that reflect the cytosolic region of a cell), and the DAPI channel ($\lambda_{\text{ex}} 365 \text{ nm}$ and $\lambda_{\text{em}} 465 \pm 35 \text{ nm}$). The data were analyzed using quantitative imaging and segmentation software (Harmony 4.9; PerkinElmer). For analysis of tumor spheroids, they were stained with either MitoTracker Red (MTR) CMXRos (ThermoFisher), sytox green (ThermoFisher), or anti-calreticulin (CRT) Alexa Fluor (AF) 647 (Novus) to assess mitochondrial activity, cell death, and immunogenic cell death, respectively. Imaging was done by using the high content imaging device with a 5x air (NA = 0.16) objective and four z-stacks per spheroid in non-confocal mode. These z-stacks of each spheroid were merged using maximum intensity projections. The spheroids area was segmented and evaluated using Harmony software for the extent of cell death (sytox green intensity per spheroid), the oxidation (MTR intensity per spheroid), and CRT expression (AF647 intensity per spheroid).

Flow cytometry

To investigate the extent of apoptosis following gas plasma irradiation, the cells were incubated with caspase 3/7 detection reagent (ThermoFisher) and DAPI. Cells were detached using accutase (BioLegend) and analyzed using flow cytometry (CytoFLEX S and LX; Beckman-Coulter). For analysis of immunogenic cell death (ICD) markers, the cells were incubated with monoclonal antibodies targeted against CRT and labeled with AF647 (Novus), heat-shock protein (HSP) 70 AF488 (BioLegend), HSP90 PE (Enzo), MHC-I PE-Cy7 (BioLegend), CD274 BV650 (BioLegend), as well as with iFluor 860 (AAT Bioquest). For the detection of intracellular antigens, the cells were fixed and permeabilized (fixation and permeabilization wash buffer; BioLegend) and stained with

antibodies targeted against LC3 AF488 (Cell Signaling), or phospho-eIF2 α labeled with AF488+ (Invitrogen; conjugate ThermoFisher), phospho-ATM labeled with PE (BioLegend), and ERp75 labeled with AF647+ (Santa Cruz; conjugate ThermoFisher). The cells were acquired using flow cytometry, and data analysis was performed using Kaluza 2.1.1 software (Beckman-Coulter).

Supernatant analysis

Cellular supernatants were collected 1 h and 48 h after in vitro treatment procedures. Residual cells were removed via centrifugation. ATP was detected utilizing the Luminescent ATP Detection Kit (Abcam), and luminescence was measured using a multimode plate reader (Tecan). Enzyme-linked immunosorbent assays were utilized according to the manufacturers' procedures for the quantification of HSP70 (ThermoFisher), IFN2 α , IFN γ , and IL-6 (all BioLegend). The absorbance was measured using the same multiplate reader (Tecan).

In vivo tumor model

The in vivo experiments were approved by the Shahid Beheshti University of Medical Science Animal Ethics Committee (approval number IR.SBMU.RETECH.REC.1397.1212) and were conducted at the Shahid Beheshti University. The animals were housed under standard laboratory conditions (room temperature = 23°C), with an ad libitum supply of nutrition and water, and circadian environmental control (12 h light shifts). All interventions at the animals were performed under anesthesia through the injection of ketamine and xylazine. Subcutaneous breast cancers were induced by subcutaneous injection of 5×10^5 4T1 cells (ATCC CRL-2539) in each flank of 6–7 weeks old female Balb/cF3H mice (Royan Institute). Daily gas plasma irradiations were started after the tumor diameters reached 5 mm at day 12 and were performed for 21 days in total. A helium gas-driven plasma multi-jet was utilized that was operated at 20 kHz frequency with a total input power of 1 W. The gas plasma irradiation time was 300 s per tumor and was only applied to the left tumors in the irradiation group. In order to investigate tumor growth and immune cell infiltration, a portion of the animals was sacrificed at day 36 for further downstream analysis (untreated tumor: n = 16; irradiation left and right: n = 8 each). The survival of untreated and gas plasma-irradiated animals was investigated until day 72 (untreated: n = 10; irradiation: n = 10).

Tumor growth monitoring in vivo

The tumors' greatest longitudinal and transverse diameter were measured every three days. The tumor volume was calculated using a modified ellipsoidal formula ($V_{\text{tumor}} = (d_{\text{longitudinal}} \times d_{\text{transverse}}^2)$). The tumor weight at day 36 was measured after tumor explantation via a precision balance. The tumor density was calculated to be 1.056 g/ml ($m = \rho \times V$). For all tumor growth evaluations, the calculated tumor volume was normalized to that of the corresponding initial tumor volume at day 12. Moreover, sonography

(ultrasound) was performed to measure the greatest tumor length, width, and height, as well as to identify hypo or hyperdense structures within the tissue. Representative animals were additionally analyzed via computer tomography (CT) at the Faculty of Veterinary Medicine of the University of Tehran. The calculation of three-dimensional animal reconstructions, surface rendering, and tumor volume quantification was performed with the Horos 3.3.6 medical image viewer (Horos Project).

Tissue sectioning and staining

Tissue sections of 5 μm thickness were cut and immersed in xylene and different percentages of ethanol to remove the paraffin and perform rehydration. For antigen retrieval, tissue slides were placed in citrate buffer (10 mM, PH 6.0) and were washed three times with PBS containing 1% Tween (PBS-T). Peroxidase blockade was done by adding a H₂O₂ and methanol mixture in PBS-T Tween for 30 min at room temperature, followed by a similar procedure using 3% Bovine Serum Albumin (BSA) in PBS-T. After the blocking buffer was removed, 70 μl of primary antibodies solution was added. These contained anti-mouse antibodies targeted against active caspase 3, CRT, CD4, CD8, or CD11 (all cell signaling technology). After overnight incubated at 4°C, and followed by incubation with an AF555 secondary antibody for 1 h at room temperature, Antifade Mounting Medium (Vectashield) with DAPI (LSBio) was used for nuclei staining and mounting. Slide imaging was done using the high content imaging system (Operetta CLS; PerkinElmer) in 10 z- stuck with 5 μm thickness with 20x air objective to capture DAPI and AF555 emission (λ_{ex} 505 nm and λ_{em} 553 \pm 23 nm). Quantitative image analysis was performed using Harmony 4.9 Software (PerkinElmer).

Terminal deoxynucleotidyl transferase dUTP nick end labeling (TUNEL) technology labels DNA fragmentation in the last phase of apoptosis (In Situ Cell Death Detection Kit, Fluorescein, Sigma-Aldrich). Paraffin-embedded tumor tissue sections were deparaffinized and rehydrated by immersing in xylene and different percentages of ethanol. Then, the tissue sections were pretreated with proteinase k working solution (15 $\mu\text{g}/\text{ml}$ in 10 mM Tris/HCl) as a permeabilization solution for 15 min at 37°C. Slides were rinsed three times with PBS and pretreated with 50 μl of TUNEL reaction mixture (50 μl enzyme solution mixed with 450 μl label solution) in a 37°C humidified atmosphere in the dark for 60 min. The label solution also was used as a negative control for accurate target detection. In the following, the slides were incubated with 50 μl DAPI (20 μM) for 15 min and were covered by a drop of mounting medium and cover slide. TUNEL-stained and negative control tissues were imaged and quantified, as described above. For the detection of intracellular FOXP3 and IL-17 in CD4⁺ T-cells, the tissue slides were processed as described above and later fixed and permeabilized with TBS-T, as well as Triton X-100 and FOXP3 staining buffer (BioLegend). Afterward, the

nuclei were counterstained with DAPI, and the slides were incubated with antibodies targeting CD4, FOXP3, IL-17A, and IL17F (all BioLegend). The outer tissue border region was quantified by the Harmony software by counting double-positive cells.

Results

Gas plasma irradiation generated ROS that impaired breast cancer cell growth

A helium (He) gas plasma jet was used for the treatment of human breast cancer cells (MCF-7 and MDA-MB) in the *in vitro* experiments (Figure 1a) that expels reactive oxygen and nitrogen species. In gas plasma-irradiated liquids, these species deteriorate then further to oxidants that can be

quantified more conveniently with redox chemical assays. Accordingly, a gas plasma irradiation time-dependent increase of hydrogen peroxide (H_2O_2) as a product of OH (Figure 1b), nitrite (NO_2^-) as a product of nitric oxide (Figure 1c), and hypochlorous acid (HOCl) as a product of O (Figure 1d) was observed in the gas plasma-irradiated cell culture medium. Concomitantly, a modest increase in the pH of the gas plasma-irradiated liquid was observed (Figure 1e). Next, gas plasma irradiation was applied to breast cancer cells *in vitro* (Figure 1f). The treatment led to a significant increase in terminally dead MCF-7 cells (Figure 1g), and a subsequent significant decrease in the metabolic activity of the cells was observed at 24 h and 48 h post-treatment measured in the entire well containing the cells (Figure 1h). In MDA-MB breast cancer cells, gas plasma-induced terminal cell death was more pronounced as compared to MCF-7 cells (Figure 1i), while the

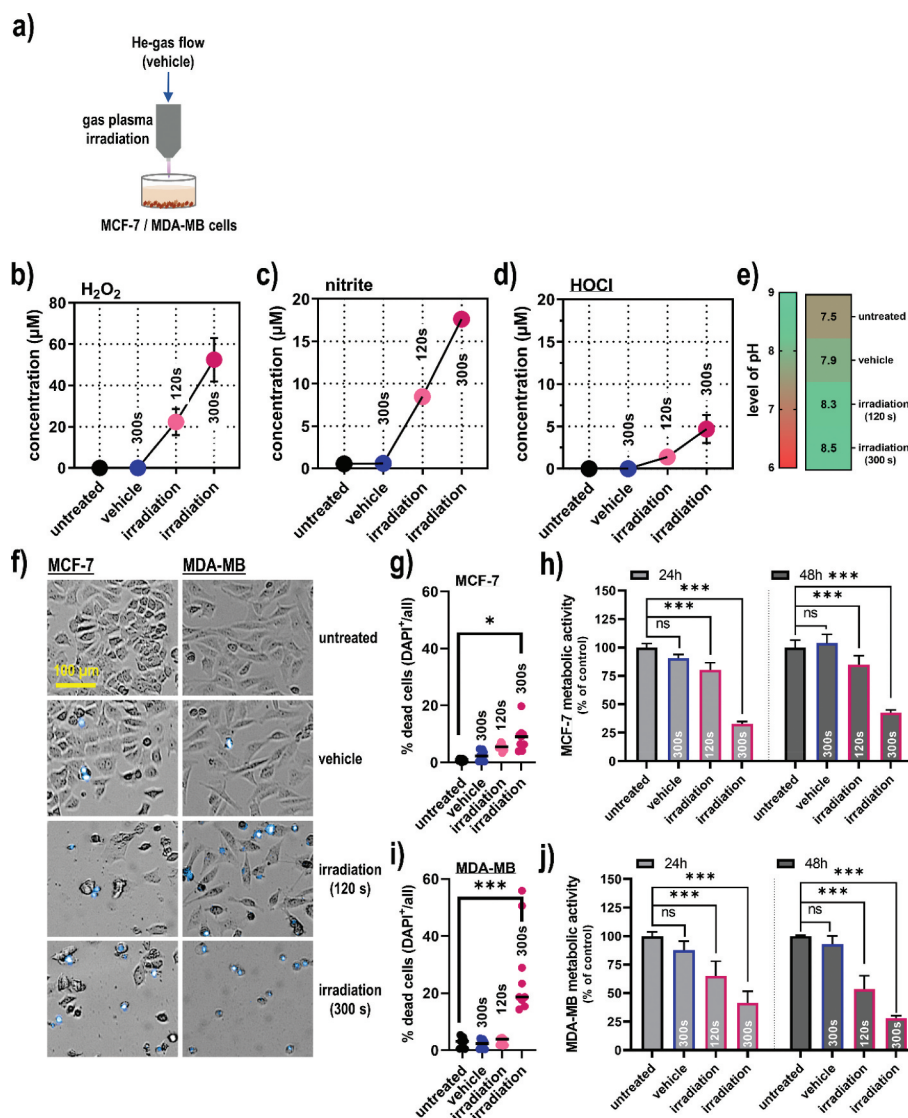


Figure 1. Gas plasma irradiation-generated redox chemistry and metabolic activity in breast cancer cells. (a) scheme of the helium (He) gas plasma irradiation of cells *in vitro*; (b-e) quantification of hydrogen peroxide (H_2O_2 , b), nitrite (NO_2^- , c), hypochlorous acid (HOCl, d), and pH (e) in gas plasma-irradiated cell culture medium; (f) representative brightfield and DAPI (terminally dead cells, blue) images of MCF-7 and MDA-MB breast cancer cells; (g) quantitative image analysis of dead cells in MCF-7 cultures; (h) metabolic activity in MCF-7 cells at 24 h and 48 h post gas plasma irradiation measured in the entire well containing the cells; (i) quantitative image analysis of dead cells in MDA-MB cultures; (j) metabolic activity in MDA-MB cells at 24 h and 48 h post gas plasma irradiation measured in the entire well containing the cells. Cell data are from three independent experiments. Data are presented as mean (\pm SD). Statistical analysis was performed using one-way analysis of variances with $p < .05$ (*) and $p < .001$ (***) ; ns = non-significant; vehicle = helium gas treatment alone (plasma ignition off); scale bar is 100 μm .

extent of reduction of metabolic activity at 24 h and 48 h post-irradiation measured in the entire well containing the cells was comparable (Figure 1j). Altogether, gas plasma irradiation generated reactive species in the gas phase and treated liquids, which subsequently reduced breast cancer cell viability and metabolic activity significantly.

Gas plasma irradiation promoted toxicity and immunogenicity in 2D and 3D cell models

To identify the mode and immunogenic consequences of gas plasma irradiation in breast cancer cells, flow cytometry was subsequently employed. In MCF-7 cells (Figure 2a), gas plasma irradiation led to a significant decline in the percentage of cells

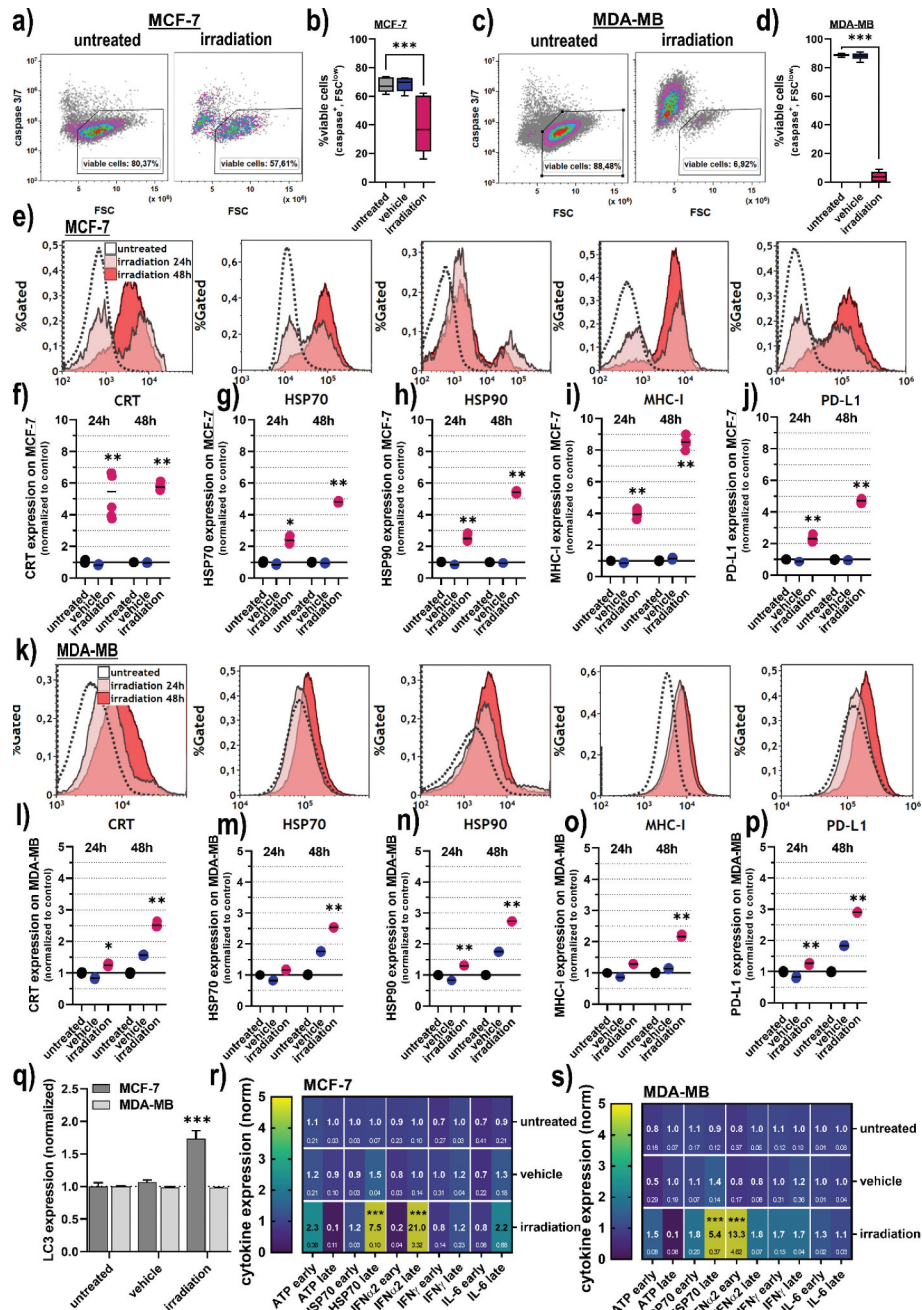


Figure 2. Cell viability and markers of immunogenic cancer cell death in breast cancer cells. (a) representative flow cytometry forward scatter (FSC) and caspase 3/7 dot-plots of MCF-7 cells; (b) quantification of viability data from flow cytometry of MCF-7 cells; (c) representative flow cytometry forward scatter (FSC) and caspase 3/7 dot-plots of MDA-MB cells; (d) quantification of viability data from flow cytometry of MDA-MB cells; (e) overlay histogram from flow cytometry of calreticulin (CRT), heat-shock protein (HSP) 70, HSP 90, major histocompatibility complex (MHC)-I, and programmed death-ligand 1 (PD-L1) in MCF-7 cells; (f-j) quantification of CRT (f), HSP70 (g), HSP90 (h), MHC-I (i), and PD-L1 (j) in viable (caspase 3/7⁻) MCF-7 cells; (k-l) overlay histogram from flow cytometry of CRT, HSP70, HSP90, MHC-I, and PD-L1 in MDA-MB cells; (l-p) quantification of CRT (l), HSP70 (m), HSP90 (n), MHC-I (o), and PD-L1 (p) in viable (caspase 3/7⁻) MDA-MB cells; (q) quantification of LC3 expression 6 h post treatment in MCF-7 and MDA-MB cells; (r-s) early (1 h) and late (48 h) cytokine expression of adenosine triphosphate (ATP), HSP70, interferon (IFN) α 2, IFN γ , and interleukin (IL)-6 in MCF-7 (r), and MDA-MB cells (s). Data are representative of at least three independent experiments and presented as mean (min-max boxplot; b,d), individual values (e-j, l-p), mean + SD (q), or mean + SEM (r-s). Statistical analysis was performed using one-way analysis of variances with $p < .05$ (*) and $p < .001$ (***).

negative for active caspases 3 and 7 (Figure 2b) being a marker of apoptosis. In MDA-MB cells (Figure 2c), a much more pronounced induction of apoptosis was observed (Figure 2d) as compared to the MCF-7 cells. The latter were subsequently analyzed for the expression of CRT, a molecule known to be increasingly expressed in cells succumbing to immunogenic cancer cell death (ICD), heat-shock-proteins (HSP) 70 and HSP90, major histocompatibility complex (MHC)-1, as well as death-ligand 1 (PD-L1) (Figure 2e). All molecules are reported to be associated with ICD and anticancer immunity,^{32–36} and a significant elevation was observed in gas plasma-irradiated but viable (caspase 3/7⁻) cells across all markers investigated (Figure 2f–j). When analyzing these markers in MDA-MB cells (Figure 2k), a significant increase of CRT was observed (Figure 2l). Also for HSP70 (Figure 2m), HSP90 (Figure 2n), MHC-I (Figure 2o), and PD-L1 (Figure 2p), significantly elevated levels were observed in gas plasma-irradiated tumor cells. In increase in the autophagy-related marker LC3, however, was observed only in MCF-7 but not MDA-MB cells (Figure 2q). As additional markers for cell death signaling, also the endoplasmic reticulum protein 57 (ERp57), the phosphorylated ATM kinase (pATM), as well as the phosphorylated eukaryotic initiation factor 2a (pEIF2a) were significantly upregulated in MCF-7, but not MDA-MB cells post-treatment Supplementary (Figure 1a–c). Besides the surface-upregulation of the ICD marker, the secretion of several inflammation and DAMP-factors cytokines was investigated in the cells' supernatants (Figure 2r–s). The levels differed when analyzed at early (1 h) versus late (48 h) collection time points. Both cell lines showed a significant increase of HSP70 as well as interferon (IFN) α 2 in the cell culture supernatant (Figure 2r–s). ATP was increased early (1 h) but not late (48 h) after gas plasma irradiation. IFN γ was only found to be increased after the treatment of MDA-MB cells but not MCF-7 (Figure 2s). In contrast, interleukin (IL)-6,

known as a general pro-inflammatory signal molecule, was elevated 48 h after exposure of MCF-7 cells to gas plasma irradiation (Figure 2r).

To confirm terminal cell death and ICD in a more realistic in vitro model, 3D tumor spheroids were generated and exposed to gas plasma irradiation (Figure 3a). In MCF-7 cells, the effect on terminal cell death (Figure 3b) and cellular oxidation (Figure 3c) was modest, while CRT expression was significantly elevated with the treatment (Figure 3d). For MDA-MB cells, a significantly increased amount of terminally dead cells was observed (Figure 3e), which was concomitant with a significant increase in intracellular oxidation (Figure 3f) and CRT (Figure 3g). The differences between both cell lines in terms of cytotoxic effects might be related to the MCF-7 cells having a more epithelial-like phenotype at the spheroids' vicinity, leading to denser 3D tumors with confined borders. The data analysis was based on the fluorescence signals from the segmented spheroids, not taking into account the viability of individual cells due to the technical limitation of unambiguously identifying all individual cells within the tumor spheroids. In summary, gas plasma irradiation induced apoptosis in human breast cancer cell lines in 2D monolayer and 3D tumor spheroid cultures, and led to a significant elevation of the molecules CRT, HSP70, HSP90, MHC-I, as well as the secretion of ATP and interferons known to be involved in ICD.

Gas plasma irradiation reduced tumor growth in vivo at the treated and remote side

The next question was whether gas plasma irradiation conferred cytotoxic and pro-immunogenic effects not only in vitro but also in vivo. For this, 4T1 syngeneic tumor cells were injected in both flanks of Balb/c mice (Figure 4a). In the control group, both tumors of each

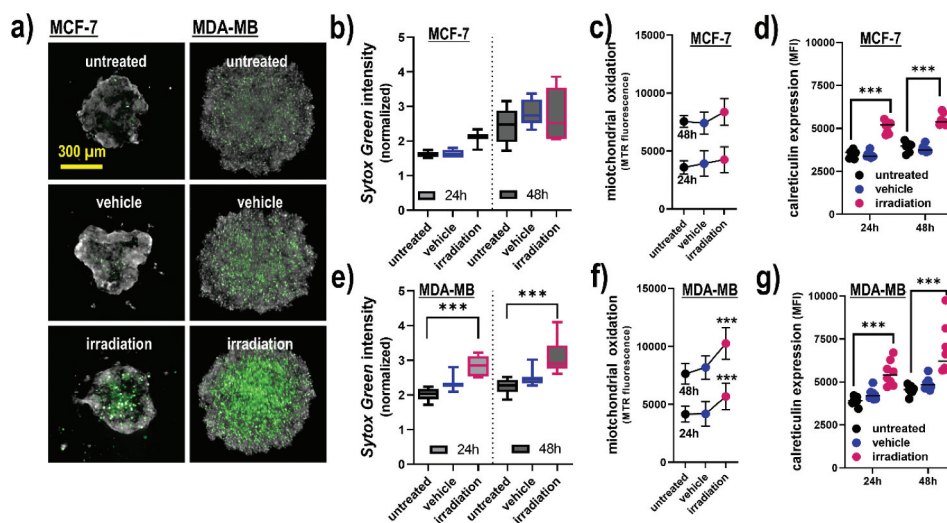


Figure 3. Viability, oxidation, and CRT expression in 3D breast cancer spheroids. (a) representative maximum intensity projection images of MCF-7 and MDA-MB 3D multicellular breast cancer spheroids generated from an overlay digital phase contrast and a sytox green image; (b–d) quantitative image analysis of the dead cell marker sytox green (b), oxidation marker mitotracker red (c), and CRT (d) of the segmented spheroid image area of MCF-7 cells at 24 h and 48 h post gas plasma irradiation exposure; (e–g) quantitative image analysis of sytox green (e), mitochondrial oxidation (f), and CRT (g) of the segmented spheroid image area of MDA-MB cells at 24 h and 48 h post gas plasma irradiation exposure. The data analysis was based on the fluorescence signals from the segmented spheroids, not taking into account the individual viability of the cells (except for sytox green). Data are from three to eight spheroids and presented as mean (min-max boxplot; \pm SD). Statistical analysis was performed using one-way analysis of variances with $p < .001$ (***); scale bar is 300 μ m.

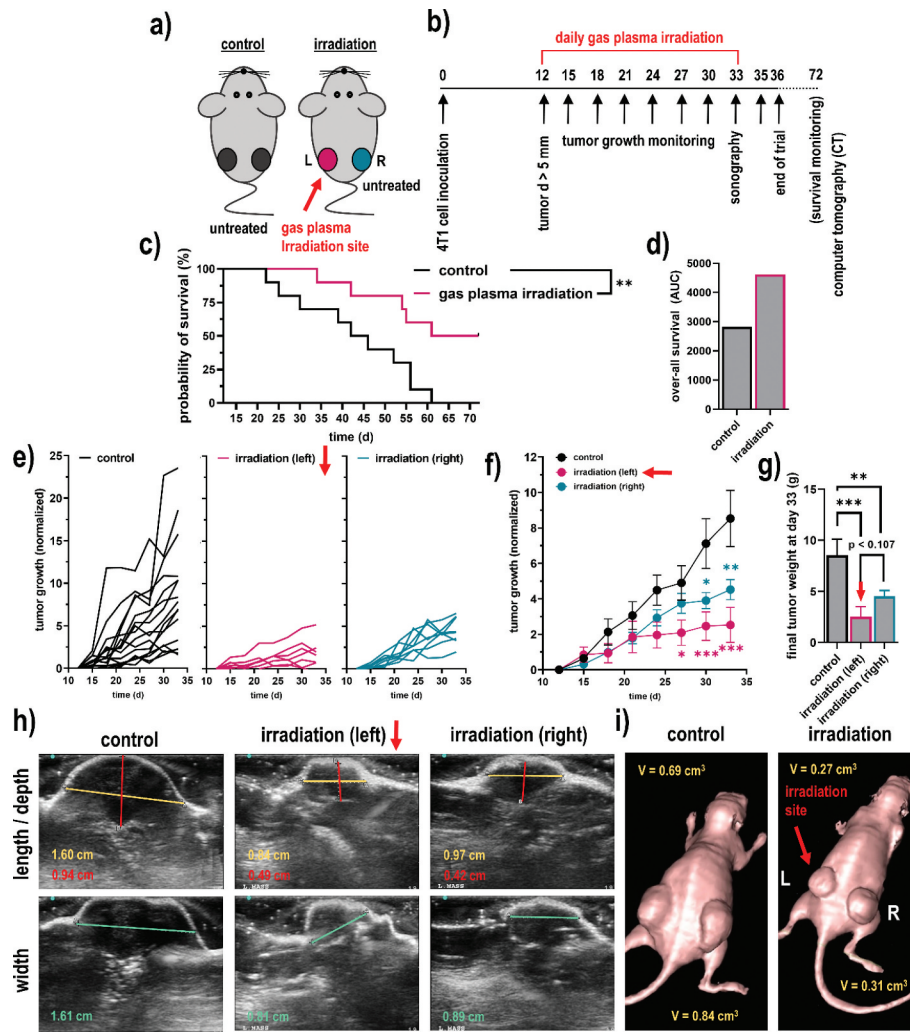


Figure 4. Syngeneic breast cancer animal model and tumor growth. (a-b) scheme of the animal treatment sides (a) and the timeline of the treatment of the breast cancer animal model (b); (c-d) Kaplan-Meier survival curve (c) and area under the curve (d) of the curves; (e) tumor sizes of individual mice of the control group (black) and the gas plasma irradiation group carrying one tumor on each flank, one being subjected to gas plasma irradiation treatment (magenta) and the tumor on the opposite side remaining untreated (turquoise); (f-g) mean tumor growth (f) and weight (g) of the untreated tumors, gas plasma irradiation-treated tumors as well as untreated opposite flank tumors of the same mice; (h-i) representative images of ultrasound (sonography) measurements of the tumors (h), and of a representative mouse of each group using computer tomography (CT). Data are from eight mice per group. Statistical analysis was performed using one-way analysis of variances with $p < .05$ (*) and $p < .01$ (**).

mouse remained untreated. In the gas plasma irradiation group, only the left tumor in each mouse was treated, while the right tumor of that same animal remained untreated. This way, we aimed at investigating remote, immune-mediated effects of the treatment on distant tumor sites following exposure to the gas plasma irradiation scheme (Figure 4b). The treatment led to a significantly increased survival in tumor-bearing mice (Figure 4c), which was overall prolonged compared to the control group (Figure 4c-d). This was also appreciated when comparing the tumor growth of the individual animals (Figure 4e) and as well as the groups (Figure 4f). Remarkably, the gas plasma irradiation not only decreased the tumor growth and weight of the directly treated breast tumor (left flank) but simultaneously, also the remote breast tumor at the opposite, non-treated side (right flank) showed a significantly impaired growth as compared to tumors of the untreated animals (Figure 4g),

suggesting distant, immune-mediated effects. The principal differences between left and right tumors in the gas plasma-irradiated group, and tumors of the control group, were confirmed using Doppler sonography (Figure 4h) and computer tomography (CT; Figure 4i). All in all, these results implicated irradiation via gas plasma technology not only to decelerate tumor growth, leading to increased survival of breast cancer-bearing mice but also to stimulate possibly immune-mediated effects resulting in impaired tumor growth at distant, untreated sites.

Gas plasma irradiation augmented immune infiltration in the tumor microenvironment

To next understand the composition of the tumor microenvironment that might be related to the antitumor effects observed with gas plasma irradiation, tissue sections were done followed by immunofluorescence staining. The quantification of positively-

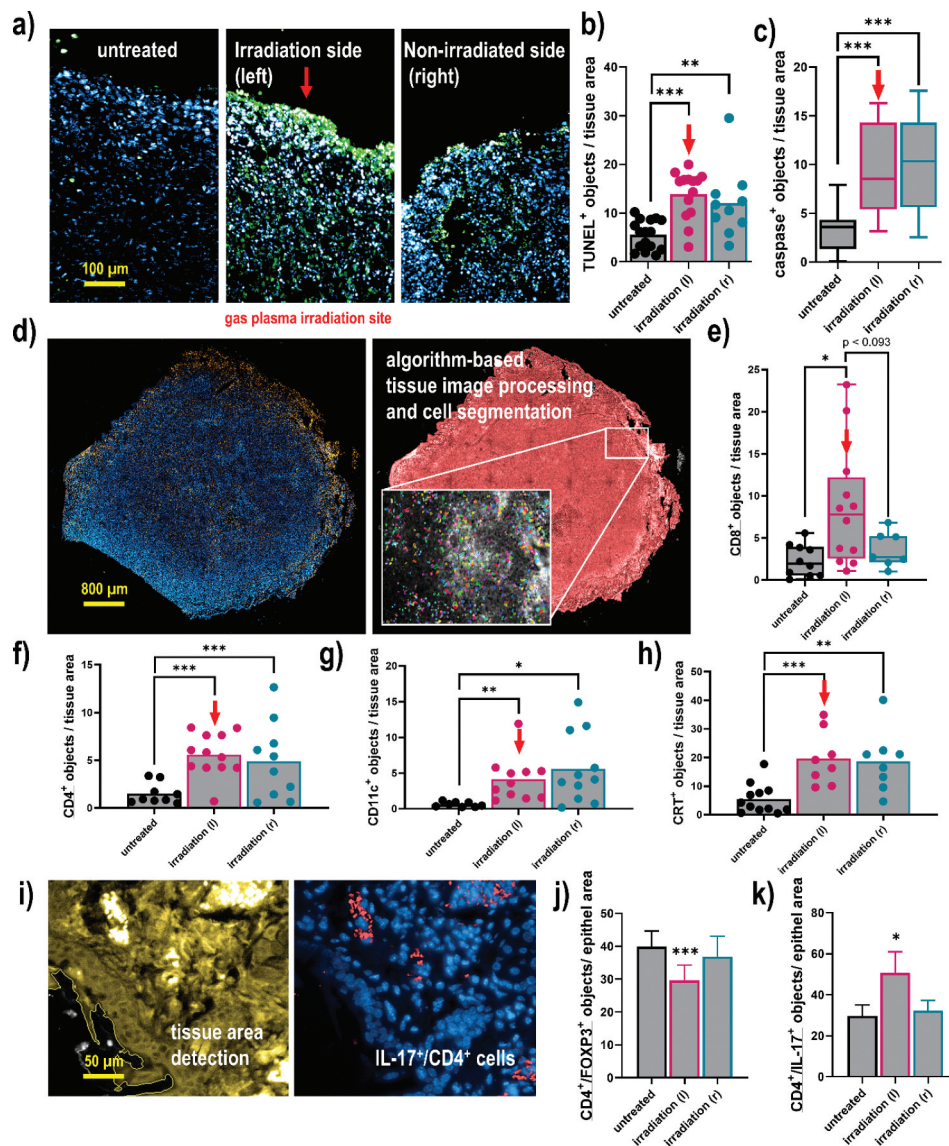


Figure 5. Quantitative imaging analysis of apoptosis, immune cell infiltrates, and CRT in breast cancer tissues. (a) representative images of tumor tissue sections stained with DAPI (nuclei, blue) for all cells and TUNEL (green) for apoptotic cells; (b-c) quantitative image analysis of TUNEL⁺ (b) and caspase 3⁺ (c) cells in tissue sections; (d) representative whole tissue section image that was stained (left) with DAPI and (blue) and anti-CD8 antibodies (orange), and segmented for different image regions (right) based on algorithm-driven image processing for unsupervised detection of cells; (e-h) quantitative image analysis results obtained for objects staining positive for CD8⁺ (e), CD4⁺ (f), CD11c⁺ (g), and CRT (h); (i) software detection of tissue border region with the quantification of (j) FOXP3⁺, and (k) IL-17⁺ subpopulations of CD4⁺ cells. The latter analysis was done for all cells staining positive for these markers, not taking into account their viability as technical limitations did not allow for such degree of multiplexing. Data show individual values and mean or min-max boxplots, or as bar graphs with mean +SEM of at least seven tumor sections per group. Statistical analysis was performed using one-way analysis of variances, or t-tests with $p < .05$ (*), $p < .01$ (**), and $p < .001$ (***) scale bars are 100 μm , 800 μm , and 50 μm , respectively.

stained cells was done using algorithm-driven image segmentation. The TUNEL staining is indicative of apoptosis (Figure 5a), and a significant increase of TUNEL⁺ cells was observed not only in gas plasma-irradiated tumors but also in opposite-flank tumors (Figure 5b). Along similar lines, the number of cells staining positive for active caspase 3, an executioner caspase of the apoptotic pathway, was significantly increased in both left and right flank tumors of gas plasma-irradiated mice when compared to untreated control tumors (Figure 5c). Subsequently, the immune infiltrate in tumor tissues was quantified (Figure 5d). For CD8⁺ cytotoxic T-cells, a significant increase was observed in the gas plasma-irradiated tumors (Figure 5e). The change in the untreated tumors of irradiated mice was modest but not significant compared to the control tumors. By contrast, the proportion of CD4⁺

T-helper cells was significantly elevated in both the gas plasma-irradiated and the opposite-flank tumor within the same animal when compared to the numbers identified in control mice (Figure 5f). A similar trend was observed for CD11⁺ cells, indicative of dendritic cells, which were significantly elevated in the gas plasma-treated mice (Figure 5g). Investigating CRT as an indicator ICD, a significantly pronounced staining was observed in both the gas plasma-treated tumors as well as the distant non-treated tumors within the same animal, when compared to those levels found in the tumors of untreated animals. Finally, when staining for subpopulations of CD4⁺ cells and quantifying their numbers in the tissues, a significantly lower amount of FOXP3⁺ CD4⁺ cells was found at the irradiation site of the animals (Figure 5i-j). IL-17 expression showed a pronounced upregulation in CD4⁺ T-cells of

the left irradiated tumor, in contrast to the opposite sided tumor and the untreated group (Figure 5k). The analysis of CD4, CD8, CD11c, CRT, FOXP3, and IL-17 was done for all cells staining positive for these markers, not taking into account their individual viability as technical limitations did not allow for such degree of multiplexing. In sum, analysis of the tumor microenvironment revealed a significant elevation of apoptosis and cell death, which was concomitant with the promotion of immunogenicity and immune cell infiltration following irradiation with gas plasma technology.

Discussion

Despite recent advances in therapy, breast cancer still is fatal in many patients. In thriving for finding novel treatment avenues, we employed an innovative medical gas plasma irradiation approach for tackling breast cancer. Treatment with this technology not only limited tumor growth in vitro and in vivo but also had an immunological dimension. Besides an upregulation of markers of the immunogenic cell death (ICD), we found in vivo untreated tumors showing decelerated growth if present in mice having tumors that had received the treatment, arguing for an abscopal effect (Figure 6).

The term abscopal effect was introduced in 1953,³⁷ describing radiotherapy of one tumor site evoking hampered growth of another, distant, untreated metastatic tumor sites. This phenomenon has occasionally been reported in the medical literature and speculated to be immune-mediated.³⁸ Today, it is well recognized

that the immune system makes a significant contribution to tumor control, as exemplified by the clinical application of check-point immunotherapy.³⁹ This understanding also sheds new light on the abscopal effect observed with predominantly local treatment, such as radiotherapy.⁴⁰ Many studies using experimental tumor models have reported abscopal effects, for instance, in pancreatic cancer,⁴¹ malignant melanoma,⁴² colon cancer,⁴³ lung cancer,⁴⁴ and breast cancer.⁴⁵ The data of our experimental model suggest gas plasma irradiation to mediate an abscopal effect, too. The distant tumor lesion responding to the local therapy usually is characterized not only by retarded growth but also an enhanced immune infiltrate, such as T-cells.⁴⁶ Especially cytotoxic CD8⁺ T-cells were in focus in recent years when it came to harnessing the power of antitumor T-cell responses.⁴⁷ This subtype, however, was not significantly enhanced in our study when investigating the tumor microenvironment (TME). By contrast, we found significantly elevated numbers of CD4⁺ T-cells in the TME, also on the gas plasma irradiated tumor site. This is of note as we previously determined T-cells to be highly susceptible to gas plasma irradiation-induced oxidative stress^{48–50} in vitro, which was predominantly found in antigen-experienced memory T-cells.⁵¹ Hence, gas plasma irradiation-induced T-cell death either is of minor relevance in vivo or not resolved kinetically as new T-cells constantly migrate into the TME from the circulation. In the current studies, the CD4⁺ T-cells expressed pro-inflammatory IL-17, while the immunosuppressive subtype was less pronounced, as FOXP3 expression suggested. CD4⁺ T cells have long been underappreciated in their ability to contribute

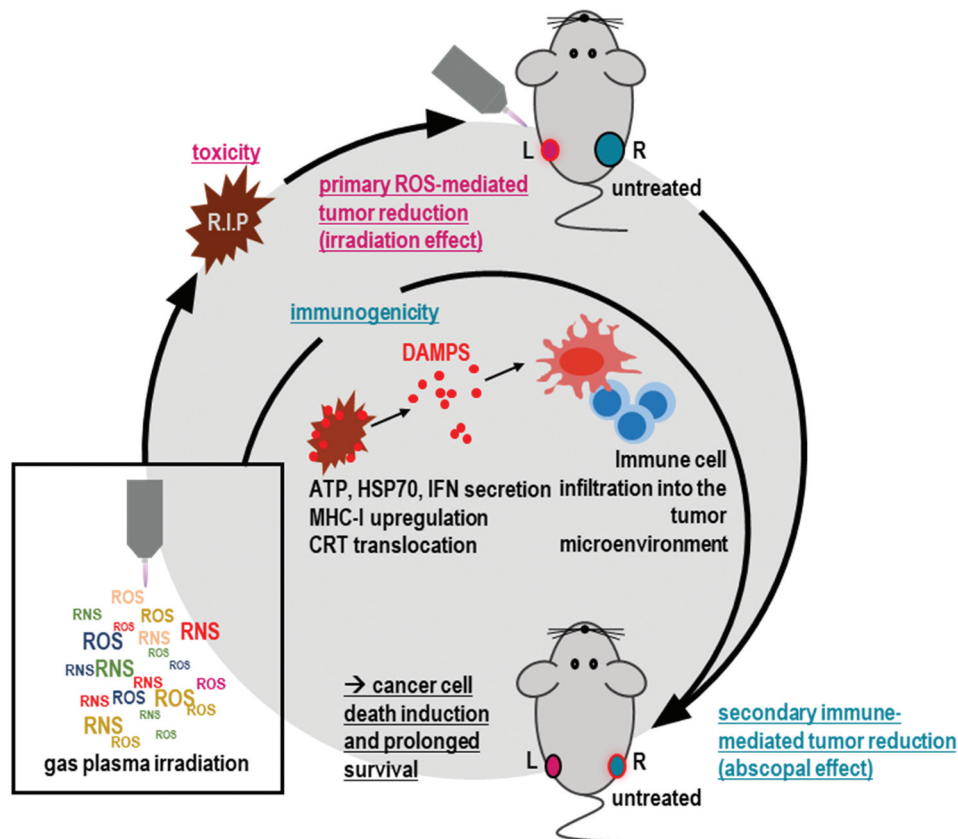


Figure 6. Scheme of gas plasma irradiation in breast cancer treatment. Gas plasma irradiation generates multiple types of ROS and RNS simultaneously, which subsequently induce cytotoxicity in breast cancer cells in vitro and in vivo. Concurrently, cell death occurs in an immunogenic fashion, leading to immune-mediated tumor reduction at a distant site not exposed to gas plasma irradiation (abscopal effect) and improved survival.

antitumor effects in the TME,⁵² albeit their positive prognostic value in cancers of, for instance, the head and neck,^{53,54} the lung,⁵⁵ and the breast.⁵⁶ The value of CD4⁺ T-helper cells lies in their supportive interplay with other types of immune cells, such as cytotoxic CD8⁺ T-cells that subsequently exert the antitumor effects in experimental models.^{57,58} The polyfunctional role of CD4⁺ T-cells is even extended to direct cytotoxic action as premature evidence points into mechanism related to MHCII-expression on tumor cells.^{59,60} CD4⁺ T-cells, moreover, promote the antitumor efficacy of dendritic cells (DCs),⁶¹ a cell type we also found to be increased in the gas plasma-irradiated breast cancers, as compared to controls.

DCs are professional antigen-presenting cells that respond to damage-associated molecular patterns (DAMPs).⁶² DAMPs are intimately linked to the immunogenic cancer cell death (ICD),³⁵ a pro-inflammatory cell death program that overrides the predominantly immunosuppressive nature of many types of regulated cell death.⁶³ In this regard, we found the DAMPs and ICD-associated molecules HSP70, HSP90, calreticulin (CRT), and MHC-I, as well as ATP secretion, IFN α 2, IFN γ , and the interleukin 6 (IL-6) to be upregulated following gas plasma irradiation. Also, the programmed death-ligand 1 (PD-L1) which contributes to a muted immune response was found to be upregulated as it is also known for radiation therapy.^{64,65} However, this might be outbalanced by the pro-inflammatory molecules that were increasingly present as well, such as CRT. CRT levels depend on the type of chemotherapeutic agent used and are associated with elevated rejection rates of tumors in vivo.²⁸ Intriguingly, also localized therapies such as ionizing radiation and photodynamic therapy (PDT) led to increased CRT levels in tumor cells and subsequently hampered tumor growth in vivo that was associated with increased immune infiltrates into the TME.^{66–69} The effects of both PDT and radiotherapy are known to be mediated significantly via reactive oxygen species (ROS).^{70–72} ROS, in turn, have significant implications in the release and appearance of DAMPs and ICD in terms of not only oxidative damage but also redox regulation.^{73–76}

Medical gas plasma systems are a novel technology for oncotherapy. Gas plasmas expel a multitude of different ROS and RNS onto the irradiated target in a localized fashion.²⁵ In contrast to radiotherapy and PDT, these reactive species are not generated inside the target cells but are being deposited from the extracellular gas plasma phase. Our results showing gas plasma irradiation-mediated cytotoxicity in breast cancer cells are in line with a previous study reporting increased apoptosis and cell damage related to antioxidant profiles and degradation of PKD2.^{77–79} Using a microcapillary plasma jet, a limitation of breast cancer growth in vivo and an increase in the number of TUNEL⁺ cells was also noted before.⁸⁰ Interestingly, gas plasma irradiation was shown to induce hallmarks of immunogenic cell death before in malignant melanoma cells,^{81,82} lung cancer,⁸³ and colorectal cancer.^{84,85} Some reports also observed ICD-induction in tumor cells exposed to cell culture medium⁸⁶ or phosphate-buffered saline⁸⁷ previously irradiated with gas plasma, implicating that some of the long-lived ROS may contribute to effects observed.⁸⁸ These

treatments were also associated with higher tumor immuno-infiltrates in vivo when applied as intraperitoneal lavage to target peritoneal carcinomatosis of colorectal or pancreatic cancer origin.^{87,89} In vivo, direct gas plasma-induced ICD was not only found to correlate with anticancer efficacy and immune infiltration^{85,90,91} but also showed protection of subsequent re-challenge using the syngeneic vaccination model with gas plasma-inactivated tumor cells.^{31,81} Along with our findings, these results suggest gas plasma irradiation to be a novel and potent tool for promoting antitumor immunity by eliciting ICD in tumor cells. An open question, however, remains, which single or composite of reactive species in terms of quantity and quality contribute to gas plasma irradiation-induced ICD. Among the species being generated, especially in our system, is, for instance, hydroxyl radicals, superoxide anion, nitrite, singlet delta oxygen, hydrogen peroxide, nitrate, atomic oxygen, nitric oxide, ozone, peroxyxynitrite, and several types of metastables, each having distinct spatio-temporal distributions and reaction kinetics with other molecules.^{92–96} While it is known that the multi-ROS nature of gas plasmas exceeds the extent of ICD when compared to individual species,⁸¹ it is also clear the individual distribution within this ROS cocktail affects ICD-related outcomes as well.³¹ The proof-of-concept of ROS-induced ICD remains exciting as a recent study had suggested increased tumor cell immunogenicity and more potent therapeutic effects of autologous DCs in patients suffering from metastatic ovarian cancer.^{97,98}

Novel cancer therapies not only need to be effective but also safe. While exact technical parameters and the type of feed gas differ between gas plasma systems, their unifying theme is the generation of ROS together with other plasma components, such as electrons and ions, electric fields, and UV-emission. A large body of evidence, however, points to ROS and RNS to be the primary mode of action.²⁵ For some gas plasma jets, extensive safety testing has been performed before.⁹⁹ This includes the absence of mutagenic effects using the OECD-accredited assays for HRPT¹⁰⁰ and micronucleus in vitro¹⁰¹ and in vivo.¹⁰² Moreover, a one-year follow-up study in mice¹⁰³ and human volunteers¹⁰⁴ did not report on any tumorigenic effects of repeated gas plasma irradiation. Moreover, gas plasma irradiation seems to target malignant over nonmalignant cells selectively.^{24,105} It is suggested that this is due to faster proliferation,¹⁰⁶ the different lipid composition of the cell plasma membrane,¹⁰⁷ lower concentration of cholesterol,¹⁰⁸ lower levels of antioxidants,¹⁰⁹ and/or higher ROS concentration in cancer cells.^{110,111} For breast cancer cells, it was speculated that their accelerated genome mutation rate, as well as hyper-activated MAPK/JNK and NF- κ B pathways, promote their vulnerability toward gas plasma irradiation when compared to nonmalignant cells.¹¹²

A limitation of our study was the lack of the gold standard prophylactic vaccination. The non-orthotopic model of breast

cancer is only partially realistic in terms of microenvironment and cellular differentiation. The blockage of effector cell subtypes and its effect on tumor growth was not investigated but cellular subtypes and tumor immuno-infiltration was analyzed.





Acknowledgments

Technical support of Lea Miebach, Grit Liebelt, Felix Niessner, Rajesh Gandhirajan and Jana Hinze, and is gratefully acknowledged. This work was supported by the German Federal Ministry of Education and Research (BMBF), grant numbers 03Z22DN11 and 03Z22Di1.

Funding

This work was supported by the German Federal Ministry of Education and Research (BMBF) [03Z22DN11]; German Federal Ministry of Education and Research (BMBF) [03Z22Di1].

ORCID

Eric Freund  <http://orcid.org/0000-0003-2950-0984>
 Udo S. Gaipf  <http://orcid.org/0000-0001-6375-5476>
 Keivan Majidzadeh-a  <http://orcid.org/0000-0002-8811-0997>
 Sander Bekeschus  <http://orcid.org/0000-0002-8773-8862>

Originality disclosure

The data presented in this manuscript are original and have not been published elsewhere.

Declaration of interest statement

The authors report no conflict of interest.

References

- Li, N.; Deng, Y.; Zhou, L.; Tian, T.; Yang, S.; Wu, Y.; Zheng, Y.; Zhai, Z.; Hao, Q.; Song, D.; Zhang, D.; Kang, H.; Dai, Z. Global burden of breast cancer and attributable risk factors in 195 countries and territories, from 1990 to 2017: Results from the global burden of disease study 2017. *J Hematol Oncol.* 2019;12:140. doi:10.1186/s13045-019-0828-0.
- Curado MP. Breast cancer in the world: incidence and mortality. *Salud Publica Mex.* 2011;53:372–384.
- Jemal A, Bray F, Center MM, Ferlay J, Ward E, Forman D. Global cancer statistics. *CA Cancer J Clin.* 2011;61:69–90. doi:10.3322/caac.20107.
- Chakraborty S, Rahman T. The difficulties in cancer treatment. *Ecancermedalscience.* 2012;6:ed16. doi:10.3332/ecancer.2012.ed16.
- Guan X. Cancer metastases: challenges and opportunities. *Acta Pharm Sin B.* 2015;5(5):402–418. doi:10.1016/j.apsb.2015.07.005.
- Coleman RE, Lipton A, Roodman GD, Guise TA, Boyce BF, Brufsky AM, Clezardin P, Croucher PI, Gralow JR, Hadji P, et al. Metastasis and bone loss: advancing treatment and prevention. *Cancer Treat Rev.* 2010;36:615–620. doi:10.1016/j.ctrv.2010.04.003.
- Falzone L, Salomone S, Libra M. Evolution of cancer pharmacological treatments at the turn of the third millennium. *Front Pharmacol.* 2018;9:1300. doi:10.3389/fphar.2018.01300.
- Mokhtari RB, Homayouni TS, Baluch N, Morgatskaya E, Kumar S, Das B, Yeger H. Combination therapy in combating cancer. *Oncotarget.* 2017;8(23):38022. doi:10.18632/oncotarget.16723.
- Pucci C, Martinelli C, Ciofani G. Innovative approaches for cancer treatment: current perspectives and new challenges. *Ecancermedalscience.* 2019;13:961. doi:10.3332/ecancer.2019.961.
- Vanneman M, Dranoff G. Combining immunotherapy and targeted therapies in cancer treatment. *Nat Rev Cancer.* 2012;12:237–251. doi:10.1038/nrc3237.
- Sudhakar A. History of cancer, ancient and modern treatment methods. *J Cancer Sci Ther.* 2009;1:1–4. doi:10.4172/1948-5956.100000e2.
- Tokumaru Y, Joyce D, Takabe K. Current status and limitations of immunotherapy for breast cancer. *Surgery.* 2020;167(3):628–630. doi:10.1016/j.surg.2019.09.018.
- Woodward WA. Building momentum for subsets of patients with advanced triple-negative breast cancer. *Lancet Oncol.* 2020;21(1):3–5. doi:10.1016/S1470-2045(19)30737-5.
- Schmid P, Rugo HS, Adams S, Schneeweiss A, Barrios CH, Iwata H, Dieras V, Henschel V, Molinero L, Chui SY, et al. Atezolizumab plus nab-paclitaxel as first-line treatment for unresectable, locally advanced or metastatic triple-negative breast cancer (impassion130): updated efficacy results from a randomised, double-blind, placebo-controlled, phase 3 trial. *Lancet Oncol.* 2020;21(1):44–59. doi:10.1016/S1470-2045(19)30689-8.
- Bhandaru M, Rotte A. Monoclonal antibodies for the treatment of melanoma: present and future strategies. *Methods Mol Biol.* 2019;1904:83–108. doi:10.1007/978-1-4939-8958-4_4.
- Berner F, Bomze D, Diem S, Ali OH, Fassler M, Ring S, Niederer R, Ackermann CJ, Baumgaertner P, Pikor N, et al. Association of checkpoint inhibitor-induced toxic effects with shared cancer and tissue antigens in non-small cell lung cancer. *JAMA Oncol.* 2019;5:1043–1047. doi:10.1001/jamaoncol.2019.0402.
- Samstein RM, Lee CH, Shoushtari AN, Hellmann MD, Shen R, Janjigian YY, Barron DA, Zehir A, Jordan EJ, Omuro A, et al. Tumor mutational load predicts survival after immunotherapy across multiple cancer types. *Nat Genet.* 2019;51:202–206. doi:10.1038/s41588-018-0312-8.
- Schumacher TN, Schreiber RD. Neoantigens in cancer immunotherapy. *Science.* 2015;348(6230):69–74. doi:10.1126/science.aaa4971.
- Ruckert M, Deloch L, Fietkau R, Frey B, Hecht M, Gaipf US. Immune modulatory effects of radiotherapy as basis for well-reasoned radioimmunotherapies. *Strahlenther Onkol.* 2018;194:509–519. doi:10.1007/s00066-018-1287-1.
- Arina A, Gutiontov SI, Weichselbaum RR. Radiotherapy and immunotherapy for cancer: from “systemic” to “multisite”. *Clin Cancer Res.* 2020. doi:10.1158/1078-0432.CCR-19-2034.
- Zhang D, Zhou T, He F, Rong Y, Lee SH, Wu S, Zuo L. Reactive oxygen species formation and bystander effects in gradient irradiation on human breast cancer cells. *Oncotarget.* 2016;7:41622–41636. doi:10.18632/oncotarget.9517.
- Pasqual-Melo G, Sagwal SK, Freund E, Gandhirajan RK, Frey B, von Woedtke T, Gaipf U, Bekeschus S. Combination of gas plasma and radiotherapy has immunostimulatory potential and additive toxicity in murine melanoma cells in vitro. *Int J Mol Sci.* 2020;21:1379. doi:10.3390/ijms21041379.
- Perillo B, Di Donato M, Pezone A, Di Zazzo E, Giovannelli P, Galasso G, Castoria G, Migliaccio A. Ros in cancer therapy: the bright side of the moon. *Exp Mol Med.* 2020;52:192–203. doi:10.1038/s12276-020-0384-2.
- Dai X, Bazaka K, Richard DJ, Thompson ERW, Ostrikov KK. The emerging role of gas plasma in oncotherapy. *Trends Biotechnol.* 2018;36:1183–1198. doi:10.1016/j.tibtech.2018.06.010.
- Privat-Maldonado A, Schmidt A, Lin A, Weltmann KD, Wende K, Bogaerts A, Bekeschus S. Ros from physical plasmas: redox chemistry for biomedical therapy. *Oxid Med Cell Longev.* 2019;2019:9062098. doi:10.1155/2019/9062098.
- Reuter S, von Woedtke T, Weltmann KD. The kinpen-a review on physics and chemistry of the atmospheric pressure plasma jet and its applications. *J Phys D: Appl Phys.* 2018;51. doi:10.1088/1361-6463/aab3ad.
- Semmler ML, Bekeschus S, Schafer M, Bernhardt T, Fischer T, Witzke K, Seebauer C, Rebl H, Grambow E, Vollmar B, et al. Molecular mechanisms of the efficacy of cold atmospheric pressure

- plasma (cap) in cancer treatment. *Cancers (Basel)*. 2020;12(2):269. doi:10.3390/cancers12020269.
28. Obeid M, Tesniere A, Ghiringhelli F, Fimia GM, Apetoh L, Perfettini JL, Castedo M, Mignot G, Panaretakis T, Casares N, *et al*. Calreticulin exposure dictates the immunogenicity of cancer cell death. *Nat Med*. 2007;13:54–61. doi:10.1038/nm1523.
 29. Garg AD, Agostinis P. Cell death and immunity in cancer: from danger signals to mimicry of pathogen defense responses. *Immunol Rev*. 2017;280:126–148. doi:10.1111/imr.12574.
 30. Hasse S, Meder T, Freund E, von Woedtke T, Bekeschus S. Plasma treatment limits human melanoma spheroid growth and metastasis independent of the ambient gas composition. *Cancers (Basel)*. 2020;12(9):2570. doi:10.3390/cancers12092570.
 31. Bekeschus S, Clemen R, Niessner F, Sagwal SK, Freund E, Schmidt A. Medical gas plasma jet technology targets murine melanoma in an immunogenic fashion. *Adv Sci (Weinh)*. 2020;7:1903438. doi:10.1002/advs.201903438.
 32. Fucikova J, Moserova I, Truxova I, Hermanova I, Vancurova I, Partlova S, Fialova A, Sojka L, Cartron PF, Houska M, *et al*. High hydrostatic pressure induces immunogenic cell death in human tumor cells. *Int J Cancer*. 2014;135:1165–1177. doi:10.1002/ijc.28766.
 33. Fucikova J, Kralikova P, Fialova A, Brtnicky T, Rob L, Bartunkova J, Spisek R. Human tumor cells killed by anthracyclines induce a tumor-specific immune response. *Cancer Res*. 2011;71(14):4821–4833. doi:10.1158/0008-5472.CAN-11-0950.
 34. Cirone M, Di Renzo L, Lotti LV, Conte V, Trivedi P, Santarelli R, Gonnella R, Frati L, Faggioni A. Primary effusion lymphoma cell death induced by bortezomib and ag 490 activates dendritic cells through cd91. *PLoS One*. 2012;7:e31732. doi:10.1371/journal.pone.0031732.
 35. Galluzzi L, Buque A, Kepp O, Zitvogel L, Kroemer G. Immunogenic cell death in cancer and infectious disease. *Nat Rev Immunol*. 2017;17:97–111. doi:10.1038/nri.2016.107.
 36. Ledford H, Else H, Warren M. Cancer immunologists scoop medicine nobel prize. *Nature*. 2018;562(7725):20–21. doi:10.1038/d41586-018-06751-0.
 37. Mole RH. Whole body irradiation; radiobiology or medicine? *Br J Radiol*. 1953;26:234–241. doi:10.1259/0007-1285-26-305-234.
 38. Ehlers G, Fridman M. Abscopal effect of radiation in papillary adenocarcinoma. *Br J Radiol*. 1973;46:220–222. doi:10.1259/0007-1285-46-543-220.
 39. Topalian SL, Taube JM, Pardoll DM. Neoadjuvant checkpoint blockade for cancer immunotherapy. *Science*. 2020;367. doi:10.1126/science.aax0182.
 40. Frey B, Rubner Y, Wunderlich R, Weiss EM, Pockley AG, Fietkau R, Gaipl US. Induction of Abscopal Anti-tumor Immunity and Immunogenic Tumor Cell Death by Ionizing Irradiation - Implications for Cancer Therapies. *Curr Med Chem*. 1751-1764;2012(19). doi:10.2174/092986712800099811.
 41. Schroter P, Hartmann L, Osen W, Baumann D, Offringa R, Eisel D, Debus J, Eichmuller SB, Rieken S. Radiation-induced alterations in immunogenicity of a murine pancreatic ductal adenocarcinoma cell line. *Sci Rep*. 2020;10:686. doi:10.1038/s41598-020-57456-2.
 42. Park SS, Dong H, Liu X, Harrington SM, Krco CJ, Grams MP, Mansfield AS, Furutani KM, Olivier KR, Kwon ED. Pd-1 restrains radiotherapy-induced abscopal effect. *Cancer Immunol Res*. 2015;3(6):610–619. doi:10.1158/2326-6066.CIR-14-0138.
 43. Shiraishi K, Ishiwata Y, Nakagawa K, Yokochi S, Taruki C, Akuta T, Ohtomo K, Matsushima K, Tamatani T, Kanegasaki S. Enhancement of antitumor radiation efficacy and consistent induction of the abscopal effect in mice by eci301, an active variant of macrophage inflammatory protein-1alpha. *Clin Cancer Res*. 2008;14(4):1159–1166. doi:10.1158/1078-0432.CCR-07-4485.
 44. Yin L, Xue J, Li R, Zhou L, Deng L, Chen L, Zhang Y, Li Y, Zhang X, Xiu W, *et al*. Effect of low-dose radiotherapy on abscopal responses to hypofractionated radiotherapy and anti-pd1 in mice and nscl patients. *Int J Radiat Oncol Biol Phys*. 2020. doi:10.1016/j.ijrobp.2020.05.002.
 45. Hu ZI, McArthur HL, Ho AY. The abscopal effect of radiation therapy: what is it and how can we use it in breast cancer? *Curr Breast Cancer Rep*. 2017;9:45–51. doi:10.1007/s12609-017-0234-y.
 46. Grass GD, Krishna N, Kim S. The immune mechanisms of abscopal effect in radiation therapy. *Curr Probl Cancer*. 2016;40:10–24. doi:10.1016/j.crrprobcancer.2015.10.003.
 47. Durgeau A, Virk Y, Corgnac S, Mami-Chouaib F. Recent advances in targeting cd8 t-cell immunity for more effective cancer immunotherapy. *Front Immunol*. 2018;9:14. doi:10.3389/fimmu.2018.00014.
 48. Bekeschus S, Masur K, Kolata J, Wende K, Schmidt A, Bundscherer L, Barton A, Kramer A, Broker B, Weltmann KD. Human mononuclear cell survival and proliferation is modulated by cold atmospheric plasma jet. *Plasma Process Polym*. 2013;10:706–713. doi:10.1002/ppap.201300008.
 49. Bekeschus S, von Woedtke T, Kramer A, Weltmann K-D, Masur K. Cold physical plasma treatment alters redox balance in human immune cells. *Plasma Med*. 2013;3:267–278. doi:10.1615/PlasmaMed.2014011972.
 50. Bekeschus S, Kolata J, Winterbourn C, Kramer A, Turner R, Weltmann KD, Broker B, Masur K. Hydrogen peroxide: A central player in physical plasma-induced oxidative stress in human blood cells. *Free Radic Res*. 2014;48:542–549. doi:10.3109/10715762.2014.892937.
 51. Bekeschus S, Rödder K, Schmidt A, Stope MB, von Woedtke T, Miller V, Fridman A, Weltmann K-D, Masur K, Metelmann H-R, *et al*. Cold physical plasma selects for specific t helper cell subsets with distinct cells surface markers in a caspase-dependent and nf-kb-independent manner. *Plasma Process Polym*. 2016;13:1144–1150. doi:10.1002/ppap.201600080.
 52. Zanetti M. Tapping cd4 t cells for cancer immunotherapy: the choice of personalized genomics. *J Immunol*. 2015;194:2049–2056. doi:10.4049/jimmunol.1402669.
 53. Badoual C, Hans S, Rodriguez J, Peyrard S, Klein C, Agueznay Nel H, Mosseri V, Laccourreye O, Bruneval P, Fridman WH, *et al*. Prognostic value of tumor-infiltrating cd4+ t-cell subpopulations in head and neck cancers. *Clin Cancer Res*. 2006;12:465–472. doi:10.1158/1078-0432.CCR-05-1886.
 54. de Ruiter EJ, Ooft ML, Devriese LA, Willems SM. The prognostic role of tumor infiltrating t-lymphocytes in squamous cell carcinoma of the head and neck: A systematic review and meta-analysis. *Oncoimmunology*. 2017;6:e1356148. doi:10.1080/2162402X.2017.1356148.
 55. Geng Y, Shao Y, He W, Hu W, Xu Y, Chen J, Wu C, Jiang J. Prognostic role of tumor-infiltrating lymphocytes in lung cancer: A meta-analysis. *Cell Physiol Biochem*. 2015;37(4):1560–1571. doi:10.1159/000438523.
 56. Matsumoto H, Thike AA, Li H, Yeong J, Koo SL, Dent RA, Tan PH, Iqbal J. Increased cd4 and cd8-positive t cell infiltrate signifies good prognosis in a subset of triple-negative breast cancer. *Breast Cancer Res Treat*. 2016;156:237–247. doi:10.1007/s10549-016-3743-x.
 57. Antony PA, Piccirillo CA, Akpınarli A, Finkelstein SE, Speiss PJ, Surman DR, Palmer DC, Chan CC, Klebanoff CA, Overwijk WW, *et al*. Cd8+ t cell immunity against a tumor/self-antigen is augmented by cd4+ t helper cells and hindered by naturally occurring t regulatory cells. *J Immunol*. 2005;174:2591–2601. doi:10.4049/jimmunol.174.5.2591.
 58. Bos R, Sherman LA. Cd4+ t-cell help in the tumor milieu is required for recruitment and cytolytic function of cd8+ t lymphocytes. *Cancer Res*. 2010;70:8368–8377. doi:10.1158/0008-5472.CAN-10-1322.
 59. Tay RE, Richardson EK, Toh HC. Revisiting the role of cd4(+) t cells in cancer immunotherapy-new insights into old paradigms. *Cancer Gene Ther*. 2020. doi:10.1038/s41417-020-0183-x.
 60. Mucida D, Husain MM, Muroi S, van Wijk F, Shinnakasu R, Naoe Y, Reis BS, Huang Y, Lambolez F, Docherty M, *et al*. Transcriptional reprogramming of mature cd4(+) helper t cells generates distinct mhc class ii-restricted cytotoxic t lymphocytes. *Nat Immunol*. 2013;14:281–289. doi:10.1038/ni.2523.

61. Aarntzen EH, De Vries IJ, Lesterhuis WJ, Schuurhuis D, Jacobs JF, Bol K, Schreiber G, Mus R, De Wilt JH, Haanen JB, *et al.* Targeting cd4(+) t-helper cells improves the induction of antitumor responses in dendritic cell-based vaccination. *Cancer Res.* 2013;73:19–29. doi:10.1158/0008-5472.CAN-12-1127.
62. Krysko DV, Garg AD, Kaczmarek A, Krysko O, Agostinis P, Vandenabeele P. Immunogenic cell death and damp in cancer therapy. *Nat Rev Cancer.* 2012;12:860–875. doi:10.1038/nrc3380.
63. Garg AD, Dudek AM, Agostinis P. Cancer immunogenicity, danger signals, and damp: what, when, and how? *BioFactors.* 2013;39(4):355–367. doi:10.1002/biof.1125.
64. Schulz D, Stancev I, Sorrentino A, Menevse AN, Beckhove P, Brockhoff G, Hautmann MG, Reichert TE, Bauer RJ, Ettl T. Increased pd-1l expression in radioresistant hnscc cell lines after irradiation affects cell proliferation due to inactivation of gsk-3beta. *Oncotarget.* 2019;10:573–583. doi:10.18632/oncotarget.26542.
65. Wu CT, Chen WC, Chang YH, Lin WY, Chen MF. The role of pd-1l in the radiation response and clinical outcome for bladder cancer. *Sci Rep.* 2016;6:19740. doi:10.1038/srep19740.
66. Golden EB, Frances D, Pellicciotta I, Demaria S, Helen Barcellos-Hoff M, Formenti SC. Radiation fosters dose-dependent and chemotherapy-induced immunogenic cell death. *Oncoimmunology.* 2014;3(4):e28518. doi:10.4161/onci.28518.
67. Golden EB, Apetoh L. Radiotherapy and immunogenic cell death. *Semin Radiat Oncol.* 2015;25:11–17. doi:10.1016/j.semradonc.2014.07.005.
68. Panzarini E, Inguscio V, Dini L. Immunogenic cell death: can it be exploited in photodynamic therapy for cancer? *Biomed Res Int.* 2013, 2013:482160. doi:10.1155/2013/482160.
69. Tanaka M, Kataoka H, Yano S, Sawada T, Akashi H, Inoue M, Suzuki S, Inagaki Y, Hayashi N, Nishie H, *et al.* Immunogenic cell death due to a new photodynamic therapy (pdt) with glycoconjugated chlorin (g-chlorin). *Oncotarget.* 2016;7(30):47242–47251. doi:10.18632/oncotarget.9725.
70. Dolmans DE, Fukumura D, Jain RK. Photodynamic therapy for cancer. *Nat Rev Cancer.* 2003;3:380–387. doi:10.1038/nrc1071.
71. Sonveaux P. Ros and radiotherapy: more we care. *Oncotarget.* 2017;8(22):35482–35483. doi:10.18632/oncotarget.16613.
72. Chen HHW, Kuo MT. Improving radiotherapy in cancer treatment: promises and challenges. *Oncotarget.* 2017;8(37):62742–62758. doi:10.18632/oncotarget.18409.
73. Carta S, Castellani P, Delfino L, Tassi S, Vene R, Rubartelli A. Damps and inflammatory processes: the role of redox in the different outcomes. *J Leukoc Biol.* 2009;86:549–555. doi:10.1189/jlb.1008598.
74. Castellani P, Balza E, Rubartelli A. Inflammation, damp, tumor development, and progression: A vicious circle orchestrated by redox signaling. *Antioxid Redox Signal.* 2014;20:1086–1097. doi:10.1089/ars.2012.5164.
75. Li G, Tang D, Lotze MT. Menage a trois in stress: damp, redox and autophagy. *Semin Cancer Biol.* 2013;23:380–390. doi:10.1016/j.semcancer.2013.08.002.
76. Rubartelli A, Lotze MT. Inside, outside, upside down: damage-associated molecular-pattern molecules (damp) and redox. *Trends Immunol.* 2007;28(10):429–436. doi:10.1016/j.it.2007.08.004.
77. Bekeschus S, Eisenmann S, Sagwal SK, Bodnar Y, Moritz J, Poschkamp B, Stoffels I, Emmert S, Madesh M, Weltmann KD, *et al.* Xct (slc7a11) expression confers intrinsic resistance to physical plasma treatment in tumor cells. *Redox Biol.* 2020;30:101423. doi:10.1016/j.redox.2019.101423.
78. Ninomiya K, Ishijima T, Imamura M, Yamahara T, Enomoto H, Takahashi K, Tanaka Y, Uesugi Y, Shimizu N. Evaluation of extra- and intracellular oh radical generation, cancer cell injury, and apoptosis induced by a non-thermal atmospheric-pressure plasma jet. *J Phys D: Appl Phys.* 2013;46:425401. doi:10.1088/0022-3727/46/42/425401.
79. Bekeschus S, Lippert M, Diepold K, Chiosis G, Seufferlein T, Azoitei N. Physical plasma-triggered ros induces tumor cell death upon cleavage of hsp90 chaperone. *Sci Rep.* 2019;9:4112. doi:10.1038/s41598-019-38580-0.
80. Mirpour S, Piroozmand S, Soleimani N, Jalali Faharani N, Ghomi H, Fotovat Eskandari H, Sharifi AM, Mirpour S, Eftekhari M, Nikkhah M. Utilizing the micron sized non-thermal atmospheric pressure plasma inside the animal body for the tumor treatment application. *Sci Rep.* 2016;6:29048. doi:10.1038/srep29048.
81. Lin A, Gorbanev Y, De Backer J, Van Loenhout J, Van Boxem W, Lemiere F, Cos P, Dewilde S, Smits E, Bogaerts A. Non-thermal plasma as a unique delivery system of short-lived reactive oxygen and nitrogen species for immunogenic cell death in melanoma cells. *Adv Sci (Weinh).* 2019;6:1802062. doi:10.1002/advs.201802062.
82. Bekeschus S, Rodder K, Fregin B, Otto O, Lippert M, Weltmann KD, Wende K, Schmidt A, Gandhirajan RK. Toxicity and immunogenicity in murine melanoma following exposure to physical plasma-derived oxidants. *Oxid Med Cell Longev.* 2017;2017:4396467. doi:10.1155/2017/4396467.
83. Lin A, Truong B, Patel S, Kaushik N, Choi EH, Fridman G, Fridman A, Miller V. Nanosecond-pulsed dbd plasma-generated reactive oxygen species trigger immunogenic cell death in a549 lung carcinoma cells through intracellular oxidative stress. *Int J Mol Sci.* 2017;18:966. doi:10.3390/ijms18050966.
84. Bekeschus S, Mueller A, Miller V, Gaipf U, Weltmann K-D. Physical plasma elicits immunogenic cancer cell death and mitochondrial singlet oxygen. *IEEE Transactions on Radiation and Plasma Medical Sciences.* 2018;2(2):138–146. doi:10.1109/trpms.2017.2766027.
85. Lin AG, Xiang B, Merlino DJ, Baybutt TR, Sahu J, Fridman A, Snook AE, Miller V. Non-thermal plasma induces immunogenic cell death in vivo in murine CT26 colorectal tumors. *Oncoimmunology.* 2018;7(9):e1484978. doi:10.1080/2162402X.2018.1484978.
86. Azzariti A, Iacobazzi RM, Di Fonte R, Porcelli L, Gristina R, Favia P, Fracassi F, Trizio I, Silvestris N, Guida G, *et al.* Plasma-activated medium triggers cell death and the presentation of immune activating danger signals in melanoma and pancreatic cancer cells. *Sci Rep.* 2019;9:4099. doi:10.1038/s41598-019-40637-z.
87. Freund E, Liedtke KR, van der Linde J, Metelmann HR, Heidecke CD, Partecke LI, Bekeschus S. Physical plasma-treated saline promotes an immunogenic phenotype in ct26 colon cancer cells in vitro and in vivo. *Sci Rep.* 2019;9:634. doi:10.1038/s41598-018-37169-3.
88. Bekeschus S, Schmidt A, Niessner F, Gerling T, Weltmann KD, Wende K. Basic research in plasma medicine - a throughput approach from liquids to cells. *J Vis Exp.* 2017:e56331. doi:10.3791/56331.
89. Liedtke KR, Freund E, Hackbarth C, Heidecke C-D, Partecke L-I, Bekeschus S. A myeloid and lymphoid infiltrate in murine pancreatic tumors exposed to plasma-treated medium. *Clin Plas Med.* 2018;11:10–17. doi:10.1016/j.cpme.2018.07.001.
90. Mizuno K, Yonetamari K, Shirakawa Y, Akiyama T, Ono R. Antitumor immune response induced by nanosecond pulsed streamer discharge in mice. *J Phys D: Appl Phys.* 2017;50:12LT01. doi:10.1088/1361-6463/aa5dbb.
91. Mizuno K, Shirakawa Y, Sakamoto T, Ishizaki H, Nishijima Y, Ono R. Plasma-induced suppression of recurrent and reinoculated melanoma tumors in mice. *Ieee Trpms.* 2018;2:353–359. doi:10.1109/trpms.2018.2809673.
92. Tresp H, Hammer MU, Winter J, Weltmann KD, Reuter S. Quantitative detection of plasma-generated radicals in liquids by electron paramagnetic resonance spectroscopy. *J Phys D: Appl Phys.* 2013;46:435401. doi:10.1088/0022-3727/46/43/435401.
93. Bekeschus S, Wende K, Hefny MM, Rodder K, Jablonowski H, Schmidt A, Woedtke TV, Weltmann KD, Benedikt J. Oxygen atoms are critical in rendering thp-1 leukaemia cells susceptible to cold physical plasma-induced apoptosis. *Sci Rep.* 2017;7:2791. doi:10.1038/s41598-017-03131-y.
94. Jablonowski H, von Woedtke T. Research on plasma medicine-relevant plasma-liquid interaction: what happened in the past five years? *Clin Plas Med.* 2015;3:42–52. doi:10.1016/j.cpme.2015.11.003.

95. Winter J, Sousa JS, Sadeghi N, Schmidt-Bleker A, Reuter S, Puech V. The spatio-temporal distribution of he (23s1) metastable atoms in a mhz-driven helium plasma jet is influenced by the oxygen/nitrogen ratio of the surrounding atmosphere. *Plasma Sources Sci T.* 2015;24:25015–25025. doi:10.1088/0963-0252/24/2/025015.
96. Bekeschus S, Winterbourn CC, Kolata J, Masur K, Hasse S, Broker BM, Parker HA. Neutrophil extracellular trap formation is elicited in response to cold physical plasma. *J Leukoc Biol.* 2016;100:791–799. doi:10.1189/jlb.3A0415-165RR.
97. Chiang CL, Kandalaf LE, Tanyi J, Hagemann AR, Motz GT, Svoronos N, Montone K, Mantia-Smaldone GM, Smith L, Nisenbaum HL, et al. A dendritic cell vaccine pulsed with autologous hypochlorous acid-oxidized ovarian cancer lysate primes effective broad antitumor immunity: from bench to bedside. *Clin Cancer Res.* 2013;19(17):4801–4815. doi:10.1158/1078-0432.CCR-13-1185.
98. Tanyi JL, Bobisse S, Ophir E, Tuyaerts S, Roberti A, Genolet R, Baumgartner P, Stevenson BJ, Iseli C, Dangaj D, et al. Personalized cancer vaccine effectively mobilizes antitumor t cell immunity in ovarian cancer. *Sci Transl Med.* 2018;10. doi:10.1126/scitranslmed.aao5931.
99. Bekeschus S, Schmidt A, Weltmann K-D, von Woedtke T. The plasma jet kinpen – a powerful tool for wound healing. *Clin Plas Med.* 2016;4:19–28. doi:10.1016/j.cpme.2016.01.001.
100. Wende K, Bekeschus S, Schmidt A, Jatsch L, Hasse S, Weltmann KD, Masur K, von Woedtke T. Risk assessment of a cold argon plasma jet in respect to its mutagenicity. *Mutat Res Genet Toxicol Environ Mutagen.* 2016;798-799:48–54. doi:10.1016/j.mrgentox.2016.02.003.
101. Bekeschus S, Schmidt A, Kramer A, Metelmann HR, Adler F, von Woedtke T, Niessner F, Weltmann KD, Wende K. High throughput image cytometry micronucleus assay to investigate the presence or absence of mutagenic effects of cold physical plasma. *Environ Mol Mutagen.* 2018;59:268–277. doi:10.1002/em.22172.
102. Kluge S, Bekeschus S, Bender C, Benkhai H, Sckell A, Below H, Stope MB, Kramer A. Investigating the mutagenicity of a cold argon-plasma jet in an het-mn model. *PLoS One.* 2016;11:e0160667. doi:10.1371/journal.pone.0160667.
103. Schmidt A, Woedtke TV, Stenzel J, Lindner T, Polei S, Vollmar B, Bekeschus S. One year follow-up risk assessment in skh-1 mice and wounds treated with an argon plasma jet. *Int J Mol Sci.* 2017;18. doi:10.3390/ijms18040868.
104. Metelmann H-R, Vu TT, Do HT, Le TNB, Hoang THA, Phi TTT, Luong TML, Doan VT, Nguyen TTH, Nguyen THM, et al. Scar formation of laser skin lesions after cold atmospheric pressure plasma (cap) treatment: A clinical long term observation. *Clin Plas Med.* 2013;1:30–35. doi:10.1016/j.cpme.2012.12.001.
105. Biscop E, Lin A, Boxem WV, Loenhout JV, Backer J, Deben C, Dewilde S, Smits E, Bogaerts AA. Influence of cell type and culture medium on determining cancer selectivity of cold atmospheric plasma treatment. *Cancers.* 2019;11 Basel. doi:10.3390/cancers11091287.
106. Wang M, Holmes B, Cheng X, Zhu W, Keidar M, Zhang LG. Cold atmospheric plasma for selectively ablating metastatic breast cancer cells. *PLoS One.* 2013;8:e73741. doi:10.1371/journal.pone.0073741.
107. Van der Paal J, Neyts EC, Verlact CCW, Bogaerts A. Effect of lipid peroxidation on membrane permeability of cancer and normal cells subjected to oxidative stress. *Chem Sci.* 2016;7:489–498. doi:10.1039/c5sc02311d.
108. Van Boxem W, Van der Paal J, Gorbanev Y, Vanuytsel S, Smits E, Dewilde S, Bogaerts A. Anti-cancer capacity of plasma-treated pbs: effect of chemical composition on cancer cell cytotoxicity. *Sci Rep.* 2017;7:16478. doi:10.1038/s41598-017-16758-8.
109. Acharya A, Das I, Chandhok D, Saha T. Redox regulation in cancer: A double-edged sword with therapeutic potential. *Oxid Med Cell Longev.* 2010;3:23–34. doi:10.4161/oxim.3.1.10095.
110. Saadati F, Mahdikia H, Abbaszadeh HA, Abdollahifar MA, Khoramgah MS, Shokri B. Comparison of direct and indirect cold atmospheric-pressure plasma methods in the b16f10 melanoma cancer cells treatment. *Sci Rep.* 2018;8:7689. doi:10.1038/s41598-018-25990-9.
111. Zhou D, Shao L, Spitz DR. Reactive oxygen species in normal and tumor stem cells. In *Adv. Cancer res.*, Elsevier;. 2014; Vol. 122. 1–67. <https://www.sciencedirect.com/science/article/pii/B9780124201170000013>
112. Xiang L, Xu X, Zhang S, Cai D, Dai X. Cold atmospheric plasma conveys selectivity on triple negative breast cancer cells both in vitro and in vivo. *Free Radic Biol Med.* 2018;124:205–213. doi:10.1016/j.freeradbiomed.2018.06.001.